



OPEN ACCESS

EDITED BY

Ines Neundorff,
University of Cologne, Germany

REVIEWED BY

Reik Löser,
Helmholtz Association of German Research
Centres (HZ), Germany
Mehmet Sen,
University of Houston, United States

*CORRESPONDENCE

Hans-Georg Lerchen,
✉ hans-georg.lerchen@vincerx.com

RECEIVED 19 December 2023

ACCEPTED 06 February 2024

PUBLISHED 01 March 2024

CITATION

Rebstock A-S, Wiedmann M, Stelte-Ludwig B, Wong H, Johnson AJ, Izumi R, Hamdy A and Lerchen H-G (2024), Neutrophil elastase as a versatile cleavage enzyme for activation of $\alpha\beta3$ integrin-targeted small molecule drug conjugates with different payload classes in the tumor microenvironment.
Front. Pharmacol. 15:1358393.
doi: 10.3389/fphar.2024.1358393

COPYRIGHT

© 2024 Rebstock, Wiedmann, Stelte-Ludwig, Wong, Johnson, Izumi, Hamdy and Lerchen. This is an open-access article distributed under the terms of the [Creative Commons Attribution License \(CC BY\)](https://creativecommons.org/licenses/by/4.0/). The use, distribution or reproduction in other forums is permitted, provided the original author(s) and the copyright owner(s) are credited and that the original publication in this journal is cited, in accordance with accepted academic practice. No use, distribution or reproduction is permitted which does not comply with these terms.

Neutrophil elastase as a versatile cleavage enzyme for activation of $\alpha\beta3$ integrin-targeted small molecule drug conjugates with different payload classes in the tumor microenvironment

Anne-Sophie Rebstock¹, Mareike Wiedmann¹,
Beatrix Stelte-Ludwig¹, Harvey Wong², Amy J. Johnson²,
Raquel Izumi², Ahmed Hamdy² and Hans-Georg Lerchen^{1*}

¹Vincerx Pharma GmbH, Monheim, Germany, ²Vincerx Pharma, Inc., Palo Alto, CA, United States

Introduction: The development of bioconjugates for the targeted delivery of anticancer agents is gaining momentum after recent success of antibody drug conjugates (ADCs) in the clinic. Smaller format conjugates may have several advantages including better tumor penetration; however, cellular uptake and trafficking may be substantially different from ADCs. To fully leverage the potential of small molecule drug conjugates (SMDCs) with potent binding molecules mediating tumor homing, novel linker chemistries susceptible for efficient extracellular activation and payload release in the tumor microenvironment (TME) need to be explored.

Methods: We designed a novel class of SMDCs, which target $\alpha\beta3$ integrins for tumor homing and are cleaved by neutrophil elastase (NE), a serine protease active in the TME. A peptidomimetic $\alpha\beta3$ ligand was attached via optimized linkers composed of substrate peptide sequences of NE connected to different functional groups of various payload classes, such as camptothecins, monomethyl auristatin E, kinesin spindle protein inhibitors (KSPi) and cyclin-dependent kinase 9 inhibitors (CDK-9i).

Results: NE-mediated cleavage was found compatible with the diverse linker attachments via hindered ester bonds, amide bonds and sulfoximide bonds. Efficient and traceless release of the respective payloads was demonstrated in biochemical assays. The newly designed SMDCs were highly stable in buffer as well as in rat and human plasma. Cytotoxicity of the SMDCs in cancer cell lines was clearly dependent on NE. IC_{50} values were in the nanomolar or sub-nanomolar range across several cancer cell lines reaching similar potencies as compared to the respective payloads only in the presence of NE. *In vivo* pharmacokinetics evaluating SMDC and free payload exposures in rat and particularly the robust efficacy with good tolerability in triple negative breast and small cell lung cancer murine models demonstrate the utility of this approach for selective delivery of payloads to the tumor.

Discussion: These results highlight the broad scope of potential payloads and suitable conjugation chemistries paving the way for future SMDCs harnessing the safety features of targeted delivery approaches in combination with NE cleavage in the TME.

KEYWORDS

$\alpha\beta3$ integrin, tumor microenvironment, neutrophil elastase (NE), small molecule drug conjugate, camptothecin

1 Introduction

Following Paul Ehrlich's vision of a magic bullet ("Zauberkegel"), the development of bioconjugates for targeted delivery of anticancer agents is gaining momentum after recent success of ADCs in the clinics (Schwartz, 2004; Baah et al., 2021). Small molecule drug conjugates (SMDCs) may have several advantages, such as better tumor penetration, lack of immunogenicity and easier manufacturing (Cazzamalli et al., 2018; Zhuang et al., 2019). SMDCs may also differ from ADCs in cellular uptake and trafficking to the lysosomes; hence for SMDCs, alternatives to the traditional lysosomal payload release strategies successfully used for ADCs need to be found. To fully leverage the potential of SMDCs with potent binding molecules mediating efficient tumor homing, novel linker chemistries susceptible for efficient extracellular payload release in the TME need to be explored.

To improve tumor selectivity of cytotoxic agents and to enable treatment of aggressive cancers, we were particularly interested in SMDCs targeting $\alpha\beta3$ integrins for efficient tumor homing. $\alpha\beta3$ integrins are cell surface proteins, which are highly expressed on cancer cells and activated endothelial cells in a wide range of tumor types (Danen et al., 1994). The high expression is correlated with aggressive disease and poor prognosis for patients. These integrin receptors bind to arginine-glycine-aspartate (RGD)-containing matrix proteins and have an important function in tumor-induced angiogenesis. Inhibition of $\alpha\beta3$ integrins has been extensively explored to inhibit angiogenesis and preclinical results looked promising (Hieken et al., 1996; Wu et al., 2013; Sun et al., 2019; Ludwig et al., 2021). In clinical trials integrin inhibitors were generally well tolerated, but unfortunately, due to crosstalk with VEGF receptors, no benefit in patients with cancer was observed with these agents (Hatley et al., 2018). Nonetheless, efficient, and selective tumor homing of integrin inhibitors has been shown in imaging studies and tissue analyses (Alday-Parejo et al., 2019). Therefore, a new focus of research was to use $\alpha\beta3$ integrin ligands for delivery of cytotoxic payloads to cancer tissue (Korkmaz et al., 2008; Alloatti et al., 2012; Liu et al., 2012; Raposo Moreira Dias et al., 2019; Lerchen et al., 2022; Paulus and Sewald, 2022; Paulus et al., 2023).

We previously described a novel class of SMDCs, which target $\alpha\beta3$ integrins to deliver an optimized camptothecin payload (Lerchen et al., 2022). The peptidomimetic $\alpha\beta3$ ligand employed in the conjugates was poorly internalized upon binding; therefore, we optimized the SMDCs for extracellular cleavage and payload release in the TME. We identified neutrophil elastase (NE), a serine protease active in the TME, as an appropriate enzyme to release the optimized camptothecin payload from the SMDC. Like $\alpha\beta3$ integrins, the expression of NE is high in the stroma of many tumors, but low in normal tissues (Korkmaz et al., 2008; Raposo Moreira Dias et al.,

2019) and its expression is associated with aggressive disease and metastasis (Sato et al., 2006; Lulla et al., 2023). Preclinical data of our lead compound **1** (VIP236) (Figure 1), which is currently in a Phase 1 clinical trial for treatment of advanced solid tumors (NCT05712889), have recently been published (Lerchen et al., 2023).

A particular challenge in the design and optimization of SMDCs is to achieve highly stable parent-molecules in circulation with efficient and selective cleavage only in TME. Here, we first investigated linker variations in the SMDC **1** (VIP236) and the impact on parent-molecule stability, release of 7-ethyl camptothecin payload and cytotoxic activity *in vitro* and *in vivo*. Compound **2** was selected for extended investigations as described in this paper. Another focus of this work was to broaden the scope and show the compatibility of NE-mediated activation of SMDCs with different payload classes with a particular emphasis on the cleavage site between linker and payload. We explored linker attachments to various functional groups on different payloads presenting a variety of potential cleavage sites for NE in SMDCs, such as hindered ester bonds, amide bonds and sulfoximide bonds. After the successful proof of concept with camptothecins, the peptidomimetic $\alpha\beta3$ ligand was now attached via optimized linkers composed of substrate peptide sequences of NE to different functional groups of various payload classes, such as cyclin-dependent kinase 9 inhibitors (CDK-9i), monomethyl auristatin E (MMAE), and kinesin spindle protein inhibitors (KSPi). With each of these payloads presenting different linker attachment sites, the successful identification and characterization of lead SMDCs will be described showcasing the broad applicability of NE as versatile cleavage enzyme for a variety of drug conjugates. Stability data of respective SMDCs as well as the release of payloads in a traceless manner resulting in an NE-dependent *in vitro* cytotoxicity will be presented. Pharmacokinetic data in rat as well as *in vivo* efficacy data using xenograft models will also be shown.

2 Materials and methods

2.1 Compounds

The SMDC compounds **2**, **3**, **4**, **5**, and **6** were designed at Vincerox and synthesized in the Medicinal Chemistry Research Labs of Bayer AG, Pharmaceuticals, Wuppertal as outlined in the [Supplementary Material](#).

2.2 Cell lines and *in vitro* proliferation assay in the presence and absence of neutrophil elastase

786-O (human RCC), HT-29 (human CRC), NCI-H292 (human NSCLC), NCI-H69 (human SCLC), MX-1 (human

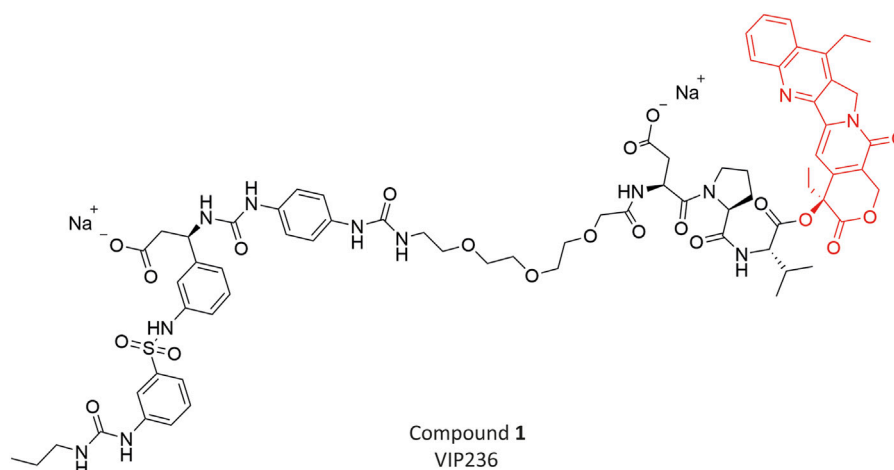


FIGURE 1
Chemical structure of Compound 1 (VIP236) with optimized CPT (Topoisomerase inhibitor) payload.

TNBC), and SUM149PT (human IBC) cells were acquired from ATCC and cultured according to the provider's instructions.

The *in vitro* cytotoxicity of the SMDCs in comparison to the respective payloads was tested in a panel of cancer cell lines after a 72 h continuous exposure in presence or absence of 20 nM neutrophil elastase using MTT assays (ATCC). IC_{50} values were determined as the concentration of compound required for 50% inhibition of cell viability.

2.3 Stability assays in buffer at pH7.4 and in rat and human plasma

The SMDC compounds **2**, **3**, **4**, **5** and **6** (1 mg) were dissolved in acetonitrile/DMSO (1:1, 0.5 mL). While vortexing, 20 μ L of this solution was added to 1 mL rat plasma at 37 °C. The incubation was stopped at respective time intervals by adding acetonitrile/buffer pH 3 (80:20) and the test compounds and formation of degradation products were analyzed by LC and LC/MS.

For hydrolytic stability measurement, compounds **2**, **3**, **4**, **5** and **6** (0.15 mg) were dissolved in acetonitrile/DMSO (4:1, 0.5 mL) and 1 mL of PBS buffer at pH 7.4 was then added. The sample solution was analyzed by HPLC to determine the amount of the test compound and the formation of degradation products over a period of 24 h at 37 °C.

2.4 Human neutrophil elastase cleavability assay

For the NE cleavability assay, the SMDC test compound was added to buffer (150 mM NaCl, 10 mM $CaCl_2$, 0.05% BSA) to a final concentration of 5 μ M (0.5% DMSO). The reaction was started by adding different concentrations of human NE (0, 20, 40, 60 nM) to the reaction vials. After incubation for 1 h at 37 °C, the enzymatic reaction was stopped by precipitation in 50% ACN. Subsequently, the samples were subjected to HPLC-MS analysis to determine the concentration of test compound and of its metabolite.

2.5 Caco-2 cell permeability assays

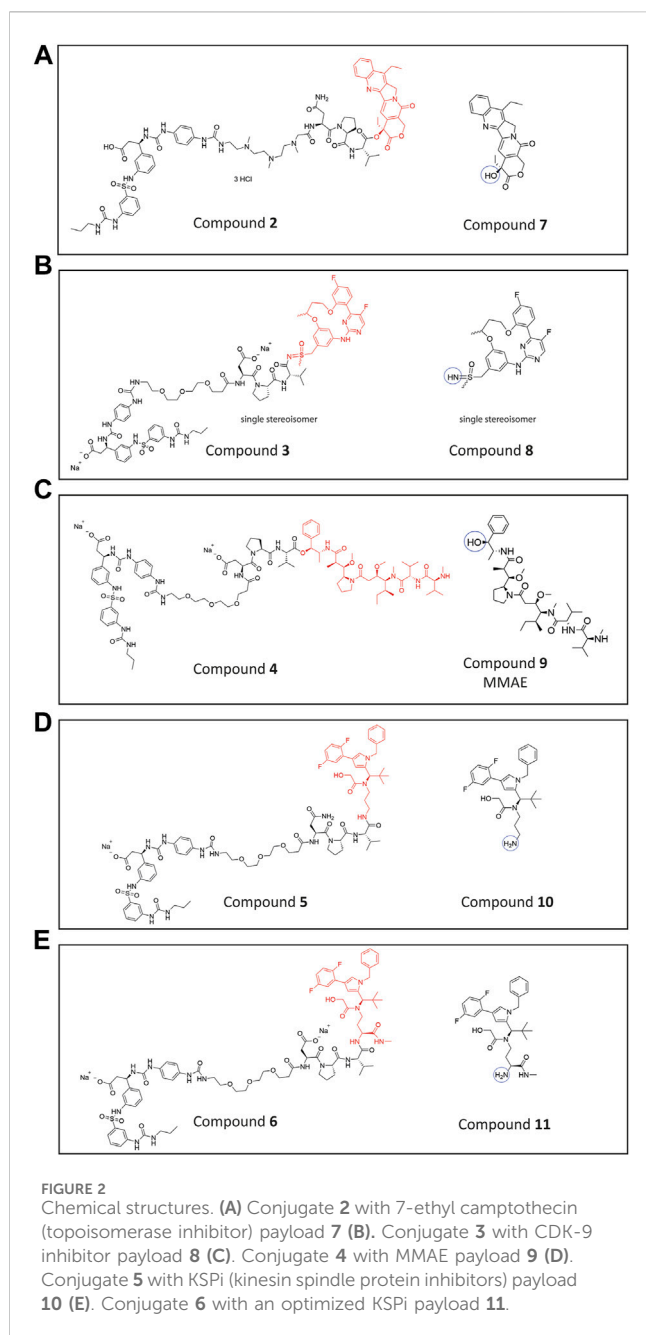
The cell permeability of the payloads released by the SMDCs **5** and **6**, namely, compounds **10** and **11** were investigated with an *in vitro* flux assay using Caco-2 cells (Troutman and Thakker, 2003). The compounds were dissolved in HEPES buffer and applied (in triplicates) to the cells either on the apical (A) or basolateral (B) side of the Caco-2 monolayer at a final concentration of 2 μ M. Before and after incubation for 2 h at 37 °C, samples were taken from both compartments and analyzed by LC-MS/MS. The apparent permeability coefficient (P_{app}) was calculated for both the apical to basolateral (A \rightarrow B) and the basolateral to apical (B \rightarrow A) direction as described by Schwab et al. (Schwab et al., 2003).

2.6 In Vivo pharmacokinetics

Pharmacokinetic properties of SMDCs and their respective payloads were characterized in rats. Briefly, male Wistar rats ($n = 3$) were given a 0.5 mg/kg dose of SMDC formulated in plasma/DMSO (99:1) intravenously (i.v.) via tail vein. Blood was collected at pre-dose, 2, 5, 15, 30, 45, 60 min, 2, 4, 7, 24 h post-dose and then processed to plasma. Plasma was frozen at $-20^{\circ}C$ until sample analysis. Plasma samples were analyzed for concentrations of SMDCs and their respective released payloads by LC-MS/MS.

In order to assess the selective concentration of payload to tumor tissue, the pharmacokinetic properties of the SMDC **3** and its payload **8**, in plasma and tumor was also characterized in female NMRI nu/nu xenograft mice (Taconic M&B A/S) bearing NCI H69 human small cell lung cancer tumors. The mice were treated i. v. via the tail vein with a single dose of **3** at 10 mg/kg. Plasma and tumor samples were collected at 0.25, 1, 7, and 24 h after treatment ($n = 2$ mice/group at each time point) and were stored frozen at $-20^{\circ}C$ until sample analysis. Concentrations of the SMDCs and their respective payloads were measured by LC-MS/MS.

Pharmacokinetics of SMDCs and their respective payloads from *in vivo* studies were determined using mean concentration-time profiles. All pharmacokinetic parameters were calculated by non-



compartmental methods as previously described (Perrier and Gibaldi, 1982).

2.7 *In vivo* efficacy in xenograft models

2.7.1 MX-1 TNBC model

For *in vivo* efficacy studies, immunocompromised mice were inoculated subcutaneously with 1×10^6 MX-1 TNBC cells in 50% Matrigel/50% Media on day 0. Treatment was started at a mean tumor volume of 75 mm^3 in the MX-1 model ($n = 12/\text{group}$: Compound **2**, 20 mg/kg i. v. in a 2 days on/5 days off and in a once weekly (QW) schedule. VIP236, 20 mg/kg i. v. QW). Tumor and body weight were measured at least twice weekly.

2.7.2 NCI H69 SCLC model

For the NCI H69 study, immunocompromised mice were inoculated subcutaneously with 1.3×10^6 NCI H69 cells in 50% Matrigel/50% Media on day 0. Treatment was started at a mean tumor area in the range of $36\text{--}37 \text{ cm}^2$ in the NCI H69 model ($n = 8/\text{group}$, compound **4** at 5 mg/kg i. v., QW, and compound **6** at 40 mg/kg i. v., QW). In an independent experiment in the same CDX xenograft model compound **3** was tested at 10 mg/kg i. v., QW. Tumor and body weight were measured at least twice weekly.

3 Results

3.1 Synthesis

The rationale of an initial study was, to replace the PEG linker in the lead compound VIP236 by a poly-amine linker and the aspartic acid in the NE-cleavable substrate sequence with asparagine to obtain an overall basic SMDC, which may be retained in the acidic TME (Dharmaratne et al., 2021). Towards this goal, compound **2** (Figure 2A) with the same 7-ethyl camptothecin payload **7** (Kunimoto et al., 1987) but with a modified linker was synthesized in a similar way as previously described for VIP236 (Lerchen et al., 2023) as outlined in the Supplementary Material.

Furthermore, we were striving for an expansion of the payloads compatible with NE-mediated activation. The peptidomimetic $\alpha\beta 3$ ligand was attached via optimized linkers composed of substrate peptide sequences of NE connected to different functional groups of various payload classes shown in Figures 2B–E, such as a CDK-9i **8** (Lücking et al., 2017), MMAE **9** (Singh, 2022) and KSPi **10** and **11** (Lerchen et al., 2018). In compound **3** (Figure 2B), the linker of VIP236 is attached to a sulfoximine group in a CDK-9 inhibitor molecule **8** (Lücking et al., 2017) instead of the 20-hydroxy group in 7-ethyl camptothecin. This is to explore whether sulfoximides may also be recognized and cleaved by NE. The CDK-9i payload **8** employed in conjugate **3** is a single stereoisomer, isolated via chiral separation. The absolute configuration of **8** was not determined. The specific stereoisomer **8** was chosen as one of the two most potent isomers out of four based on *in vitro* cytotoxicity data (data not shown). In compound **4** (Figure 2C), a novel linker attachment to the sterically hindered hydroxy group of MMAE **9** is explored. In compounds **5** and **6** (Figures 2D, E) the linker is attached to an amino group present in KSPi molecules **10** and **11** which, as previously shown, is essential and needs to be liberated from the conjugates to provide an active metabolite (Lerchen et al., 2018).

The synthesis of these SMDCs is described in the Supplementary Material.

3.2 *In vitro* cytotoxicity

The cytotoxicity of the SMDCs was measured in different cancer cell lines in the absence and presence of NE and the results are shown in Table 1.

Cytotoxicity of SMDCs in cancer cell lines was clearly dependent on NE. All SMDCs (compounds **2**, **3**, **4**, **5** and **6**) had poor cytotoxicity after incubation for 72 h in culture medium without

TABLE 1 Cytotoxicity *in vitro* in the absence and presence of elastase. IC₅₀ (M) of SMDC compounds 2, 3, 4, 5 and 6 in comparison to their corresponding payloads 7, 8, 9, 10, and 11, respectively, in 4 cell lines with and without elastase.

Compound	786–0	786–0 + neutrophil elastase	HT29	HT29 + neutrophil elastase	NCI-H292	NCI-H292 + neutrophil elastase	SUM149PT	SUM149 PT + neutrophil elastase
2	5.4E-7	3.5E-9	1.0E-6	2.0E-8	1.7E-7	6.0E-9	3.1E-7	4.8E-9
7	3.7E-9	3.2E-9	2.2E-8	1.9E-8	3.8E-9	4.6E-9	3.8E-9	4.2E-9
3	>1.0E-6	3.1E-9	9.9E-7	1.9E-9	8.8E-7	4.5E-9	7.7E-7	1.2E-9
8	4.3E-9	4.9E-9	1.7E-9	1.3E-9	2.2E-9	2.2E-9	2.3E-9	2.6E-9
4	6.6E-7	6.6E-9	7.8E-8	4.3E-10	7.1E-8	3.5E-10	5.0E-8	5.1E-10
9	5.9E-9	4.9E-9	5.8E-10	5.5E-10	4.0E-10	3.6E-10	1.8E-10	1.4E-10
5	1.0E-6	4.5E-9	1.0E-6	2.4E-9	9.9E-7	1.5E-9	3.3E-7	3.3E-10
10	2.5E-9	2.5E-9	4.1E-10	4.1E-10	4.6E-10	2.7E-10	3.3E-10	1.7E-10
6	1.0E-6	8.7E-9	1.0E-6	1.7E-9	1.0E-6	1.3E-9	1.0E-6	6.0E-10
11	6.0E-9	6.0E-9	1.2E-9	1.4E-9	1.8E-9	9.7E-10	3.1E-10	5.3E-10

NE, whereas each of the five payloads (compounds 7, 8, 9, 10 and 11) was potent in the low nanomolar or even sub-nanomolar range. These results also indicate high stability and minimal payload release from the SMDCs under these conditions. However, when NE was added to the cell culture, cytotoxicity of the SMDCs increases significantly reaching IC₅₀ values in the nanomolar or sub-nanomolar range across several cancer cell lines, thus, achieving similar potencies as compared with the respective payload alone. These results imply cleavage of the SMDCs, and release of the respective payloads mediated by NE.

3.3 Stability in buffer and in rat and human plasma

The newly designed SMDCs 2, 3, 4, 5 and 6 were highly stable in buffer, in rat and in human plasma independent of the nature of the linkage of the cytotoxic payload to the NE-cleavable linker. Data are shown in the Supplementary Figure S1.

3.4 Cleavability by human neutrophil elastase

The initial design of elastase cleavable SMDCs such as VIP236 was inspired by previous research on NE cleavable probes (Powers et al., 1977; Achilles and Bednarski, 2003). In our previous studies we have investigated VIP236 and its epimers for NE cleavability showing that the natural L-configuration of the valine residue in position P1 of the identified NE-cleavable linker aspartic acid-proline-valine is crucial for efficient payload release (Lerchen et al., 2023). The new SMDCs 2, 3, 4, 5 and 6 were investigated for cleavability by human NE in a biochemical assay at different NE concentrations. Conjugates 2, 3 and 4 were essentially completely cleaved at all tested concentrations within 60 min (Figures 3A–C). The efficient NE cleavability of the SMDCs VIP236 and 2 indicates

that there is flexibility in position P3 and beyond as the negative charge of the aspartic acid in VIP236 is not required and furthermore, a basic polyamine linker instead of a PEG linker is also tolerated. The efficient NE cleavability of SMDCs 3 and 4 is a striking finding demonstrating a broad substrate tolerance of NE particularly in the P1'–P3' region. This includes the cleavage site itself which even tolerates a switch from an ester bond in compound 2 to a sulfoximide bond in compound 3 as well as entirely different ester substrates for NE presented in SMDCs VIP236, 2 and 4. The poor *in vitro* cytotoxicity of SMDCs 2–4 (Table 1) in the absence of NE demonstrates high stability of respective SMDCs requiring NE-mediated activation of the payload. For conjugate 5, the cleavage was very slow and only small amounts of cleaved payload 10 could be detected after 60 min with the SMDC 5 remaining almost untouched. (Figure 3D). The conjugate 6 featuring an optimized KSPi payload 11 showed an improved NE-mediated cleavage increasing with higher NE concentrations (Figure 3E). These results indicate that the SAR of amide bonds to be cleaved by NE appears to be more restrictive as compared to ester bonds. Hence, NE-mediated cleavage of hindered ester bonds, amide bonds and sulfoximide bonds mediating efficient release of the respective payloads in a traceless manner was successfully demonstrated in biochemical assays.

3.5 Permeability in Caco-2 cells

Transporter pumps, such as the P-glycoprotein (P-gp) efflux pump expressed on cancer cells, are known to contribute to resistance to chemotherapy treatment (Seelig, 2020). Therefore, cellular permeability and the potential to resist efflux transporter pumps are important aspects in the selection of the antineoplastic agents to be used as the payload. The cytotoxic KSPi payloads 10 and 11 are released extracellularly from the SMDCs 5 and 6 with different kinetics. Here, we compared the permeability and efflux ratio of 10 and 11 using Caco-2 cells. 11 was approximately 10-times

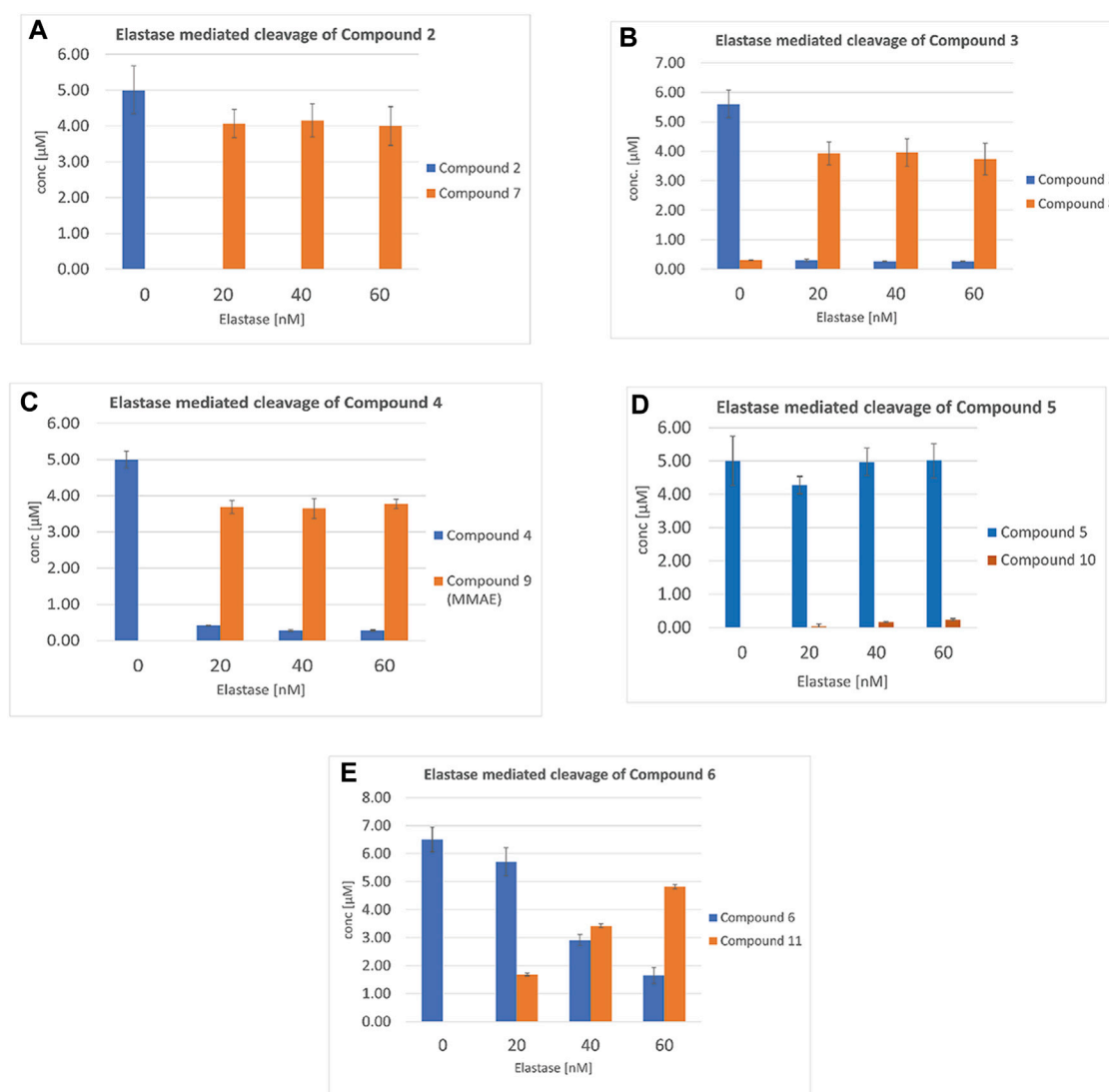


FIGURE 3 Neutrophil elastase cleavability assay of SMDCs: (A) Compound 2, (B) Compound 3, (C) Compound 4, (D) Compound 5 and (E) Compound 6 monitoring concentrations of SMDC and released payloads 7, 8, 9, 10 and 11, with 20, 40 and 60 nM NE, respectively.

more permeable than 10 (P_{app} A-B). In addition, the efflux ratio of 11 was approximately 15 times lower than 10 in Caco-2, suggesting that the compound was transported out of the cells to a much lower extent (Table 2). These results suggest conjugate 6 is releasing a payload with a significantly improved *in vitro* profile compared with conjugate 5.

3.6 *In vivo* pharmacokinetics

3.6.1 Pharmacokinetic studies in rat

To compare the pharmacokinetic properties of the SMDCs, intravenous pharmacokinetic studies were performed in rat. Plasma concentration-time profiles of the SMDCs evaluated in the rat are shown in Figure 4 and pharmacokinetic parameters are shown in Table 3. Plasma clearance of all SMDCs evaluated was low in rats with clearance being in the following rank order:

compound 3 > 5 > 2 > 6 > 4 (Table 3). Volume of distribution at steady state (V_{ss}) was low for all SMDCs being less than total body water (<0.7 L/kg) (Davies and Morris, 1993). Specifically, for SMDCs 6 and 3, the estimate of V_{ss} was comparable to plasma volume. The half-life ($t_{1/2}$) for each SMDC tended to rank in order of their respective V_{ss} estimates. The release of payload in rat plasma was low for all SMDCs evaluated with ratio of payload to parent SMDC AUC on a molar basis ≤ 0.0105 . The exception was compound 3 where the ratio of payload to parent SMDC AUC was ~ 0.31 .

3.7 *In vivo* efficacy

3.7.1 Investigation of SMDC linker variations

We sought to investigate the effect of varying the linker in the SMDC VIP236, which resulted in compound 2 with a basic poly-

TABLE 2 Permeability and efflux ratio of the payloads 10 and 11 measured in flux assays with Caco-2 cells. The values represent the mean value of at least two independent assays performed in triplicates ($n = 3$).

Compound	Caco-2 Flux P_{app} B-A	Caco-2 Flux P_{app} A-B	Caco-2 flux efflux ratio
10	179.7	3.8	129.1
11	303.0	34.8	8.7

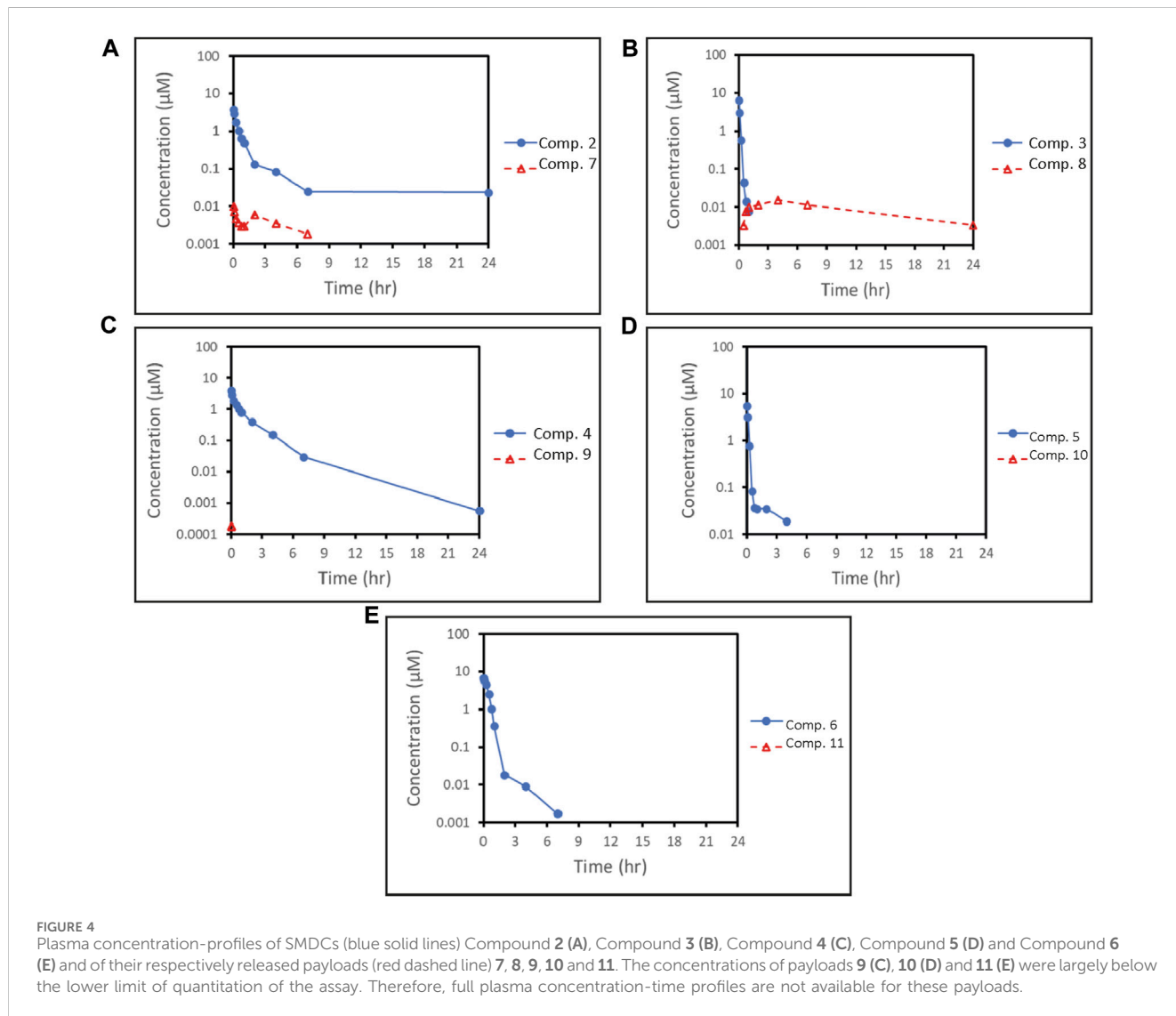
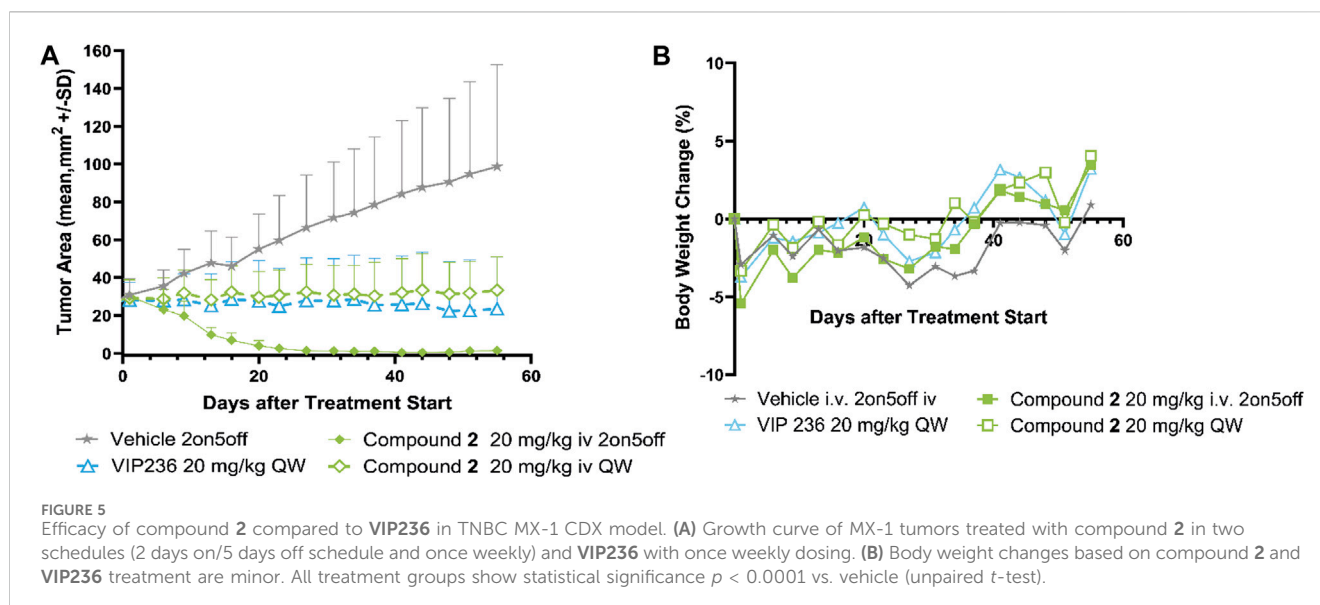


FIGURE 4 Plasma concentration–profiles of SMDCs (blue solid lines) Compound 2 (A), Compound 3 (B), Compound 4 (C), Compound 5 (D) and Compound 6 (E) and of their respectively released payloads (red dashed line) 7, 8, 9, 10 and 11. The concentrations of payloads 9 (C), 10 (D) and 11 (E) were largely below the lower limit of quantitation of the assay. Therefore, full plasma concentration–time profiles are not available for these payloads.

TABLE 3 Pharmacokinetic parameters of conjugates 2, 3, 4, 5 and 6 and release of their respective payloads.

Parameter	Compound				
	2	3	4	5	6
Cl_p (mL/min/kg)	2.33 ± 0.44	6.60 ± 0.95	1.47 ± 0.06	5.50 ± 2.35	1.69 ± 0.15
V_{ss} (L/kg)	0.627 ± 0.344	0.0366 ± 0.0053	0.157 ± 0.015	0.600 ± 0.515	0.0377 ± 0.0050
$t_{1/2}$ (h)	8.31 ± 5.49	0.240 ± 0.050	2.30 ± 0.95	4.88 ± 4.37	0.442 ± 0.023
AUC_{0-inf} ($\mu\text{mol}\cdot\text{hr/L}$)	2.52 ± 0.61	0.801 ± 0.126	3.03 ± 0.11	1.09 ± 0.49	2.98 ± 0.25
payload/parent AUC ratio	0.0105	0.307	NC	NC	NC

AUC, area under the plasma concentration–time profile; AUC_{0-inf} , area under the plasma concentration–time profile from time 0 to infinity; Cl_p , plasma clearance; $t_{1/2}$, elimination half-life; V_{ss} , volume of distribution at steady-state; NC, not calculated as warhead not detected (LLOQ < 0.0005 μM).



amine linker instead of the PEG linker used in **VIP236**. Compound 2 with the modified linker was investigated in comparison to the lead **VIP236** in the MX-1 TNBC xenograft model. Results are shown in Figures 5A, B.

Monotherapy of compound 2 demonstrated significant tumor regression in the 20 mg/kg 2on/5off schedule and was well tolerated as no significant body weight loss was observed. At a once weekly dosing of 20 mg/kg of compound 2 tumor stasis could be achieved, which was comparable to **VIP236** (Figure 5A). Based on body weight changes both compounds showed good tolerability (Figure 5B).

3.7.2 Broadening of the payload scope compatible with NE-mediated cleavage

We also sought to investigate a broadening of the payload scope and identified three different payload classes compatible with NE-mediated cleavage *in vitro*. The new SMDCs featuring a CDK-9i, MMAE, or KSPi payloads were investigated in an NCI H69 SCLC xenograft model. Initially, the SMDC 3 with the CDK-9i payload 8 was tested in the NCI H69 SCLC model with a weekly dose of 10 mg/kg in 3 treatment cycles. No significant inhibition of NCI-H69 tumor growth could be demonstrated with this dose and schedule (data not shown).

In a subsequent experiment the MMAE SMDC compound 4 and the optimized KSPi SMDC compound 6 were also evaluated in the NCI H69 xenograft model. The results are shown in Figures 6A, B.

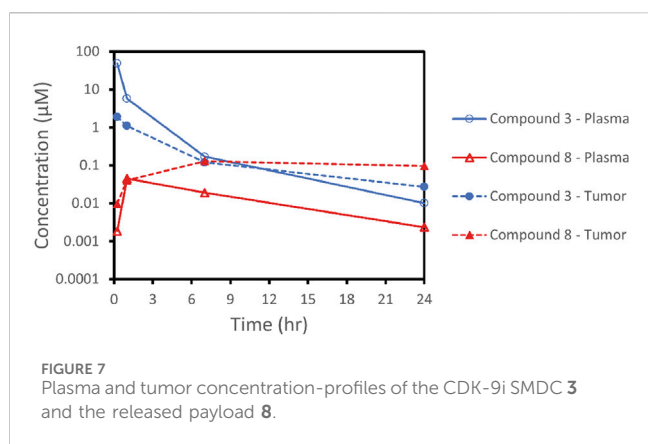
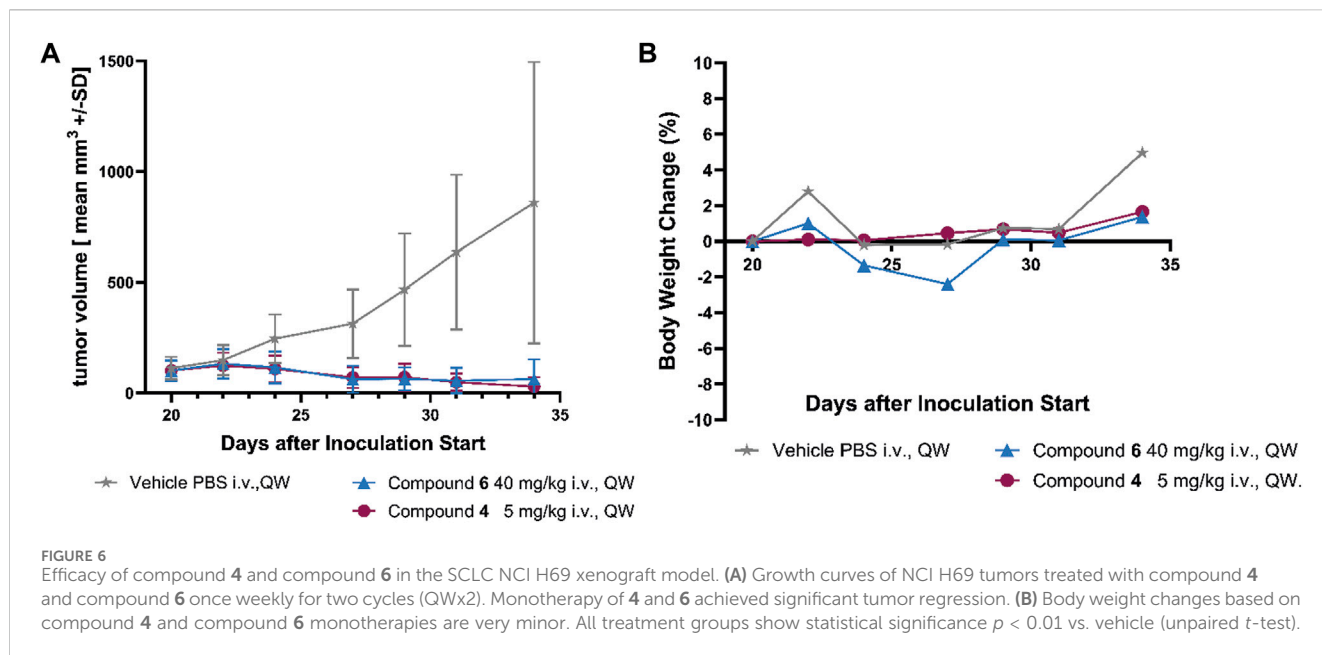
Monotherapy of SMDC 4 with MMAE as payload achieved statistically significant tumor regression with two applications of 5 mg/kg i. v. once weekly. Also, treatment with compound 6 with optimized KSPi payload at a dose of 40 mg/kg i. v. demonstrated statistically significant tumor regression with the same schedule (Figure 6A). The dosages were selected based on a previous MTD study (data not shown). Both

therapies showed a high tolerability based on the body weight changes shown in Figure 6B.

To further investigate the finding that SMDC 3 was inactive *in vivo* and to verify that delivery of SMDCs resulted in concentration of the released payload in tumor tissue as previously demonstrated for **VIP236** (Lerchen et al., 2022), a pharmacokinetic study was performed in NCI H69 tumor-bearing mice. After i. v. administration of 10 mg/kg of compound 3, plasma and tumor concentrations of the SMDC 3 and of the released payload 8 were measured; the results are shown in Figure 7 and in Table 4. The exposure of the released payload 8 was 7.6-fold higher in the tumor versus plasma, indicating a successful delivery of the free payload to tumor tissue (Table 4). Despite this nice accumulation of the CDK-9i payload 8 in tumor over plasma shown in the PK study, tumor exposures of 8 appear not to be sufficient to significantly inhibit tumor growth. Further optimization is ongoing with the goal to also demonstrate the proof of *in vivo* efficacy of SMDCs with sulfoximide-linked CDK-9i payloads for treatment of solid tumors.

4 Discussion

SMDCs are currently gaining momentum with potential advantages over ADCs, such as better tumor penetration and lack of immunogenicity (Cazzamalli et al., 2018). For the treatment of aggressive cancers, we are developing SMDCs using a peptidomimetic $\alpha v \beta 3$ integrin binder, which shows efficient tumor homing, and a linker, which is extracellularly cleaved by NE in the TME (Lerchen et al., 2022). Our lead SMDC **VIP236** (Lerchen et al., 2023) is currently in a Phase 1 clinical trial for the treatment of advanced solid tumors (NCT05712889). Preclinically, **VIP236** showed optimal activity when administered with a 2 days on/5 days off therapy schedule. Here, we show our investigations on linker variations as well



as our successful efforts to expand the payload scope in $\alpha\beta 3$ targeted SMDCs, which are susceptible to cleavage by NE. Pharmacokinetic studies in rat suggest that low clearance of the SMDC can still be maintained with changes in the payload class and linker. In addition, for most of the evaluated SMDCs, the payload/parent AUC ratio is low, suggesting stability of the linker and low systemic exposure to the payload.

4.1 Linker variation

We first explored linker variations and designed a **VIP236** analogue with the goal to improve retention in the acidic environment of the TME to potentially increase efficacy with once weekly dosing. SMDC 2 uses the same 7-ethyl camptothecin payload 7 (Kunimoto et al., 1987) as **VIP236**; however, the PEG linker present in the lead compound **VIP236** was replaced by a poly-amine linker and the aspartic acid was replaced by asparagine to obtain an overall basic SMDC, which may increase retention in the acidic TME as the SMDC will be in its protonated form (Dharmaratne et al., 2021). The *in vivo* results shown in the MX-1 TNBC model demonstrate, that 2 is a highly potent SMDC achieving complete tumor regression with a dose of 20 mg/kg administered in a 2 days on/5 days off schedule, like also previously shown with **VIP236** at a dose of 26 mg/kg in a 3 days on/5 days off schedule (Lerchen et al., 2022; Lerchen et al., 2023). At a once weekly dosing of 20 mg/kg of SMDC 2 tumor stasis could be achieved, which was comparable to **VIP236** (Figure 5A). In conclusion, the basic poly-amine linker is an alternative to the PEG linker used in **VIP236** that further broadens the modular toolbox for SMDCs.

TABLE 4 Exposures (C_{max} and AUC_{0-t}) of conjugate 3 and its respective payload 8 in plasma and tumor/plasma ratio in NCI H69 tumor bearing mice.

PK parameters	Compound 3 10 mg/kg IV	
	Conjugate 3	Payload 8
C_{max} (μM)	49	0.045
AUC_{0-t} ($\mu mol \cdot hr/L$)	43	0.33
tumor/plasma AUC ratio	0.126	7.58

AUC, area under the plasma concentration-time profile; AUC_{0-t} , area under the plasma concentration-time profile from 0 to the last timepoint; C_{max} , maximum concentration observed. LLOQ, is 0.001 μM .

4.2 Extension of payload scope

In another aspect of this work, we were striving for an expansion of the payload scope compatible with NE-mediated activation. Our focus was to investigate whether functional groups present on different payloads could be compatible with the attachment of linkers. The resulting linkage should be efficiently cleaved by NE and allow for traceless release of the payload. At the same time corresponding SMDCs should be highly stable in circulation. Raposo Moreira Dias et al. (Raposo Moreira Dias et al., 2019) described SMDCs releasing the paclitaxel payload via NE-mediated cleavage, which however, required two subsequent steps of first fragmentation and then cyclization to release the payload. The goal of our work was to use NE cleavage for direct and 'traceless' release of the respective payload avoiding further conversion steps of intermediates with different clearances. This approach may reduce complexity of DMPK and increase the efficiency of payload formation.

4.3 Monomethyl auristatin E

Protease-cleavable SMDCs using the clinically validated MMAE payload from vedotin ADCs (Senter and Sievers, 2012), with substrate sequences for cathepsin B (Bennett et al., 2020; Davis et al., 2023; Zambra et al., 2023) or legumain (Liu et al., 2012) all depend on a self-immolative para-amidobenzyloxy carbamate (PABC) moiety (Carl et al., 1981) to release the active payload MMAE. To overcome shortcomings associated with the increased hydrophobicity of such self-immolative PABC linker approaches, we were looking for alternative linker attachments enabling a traceless payload release. Due to our previous experience with NE-cleavable linkers attached to camptothecins via sterically hindered ester bonds, we investigated the hydroxy group of the nor-ephedrin amino acid present in MMAE for its suitability as a conjugation site for NE-cleavable linkers without the need for self-immolative moieties. The high stability of the ester-linked MMAE SMDC **4** *in vitro* reported in Section 3.3 nicely fits to the low levels of free payload detected in the PK studies of the SMDC in rat (Section 3.6). This stability profile in combination with the efficient and specific cleavability by NE and consequently the NE-dependent cytotoxicity of **4** demonstrate the utility of this new linker attachment site in MMAE bioconjugates to enable traceless release of the payload. Based on this profile with extracellular payload release specifically mediated by NE in a traceless manner and the high activity observed in the NCI H69 xenograft model with only two doses of 5 mg/kg administered in a once weekly schedule, the SMDC **4** represents a novel and promising option to deliver MMAE to aggressive cancers. This SMDC **4** combines excellent stability *in vivo* with high efficacy upon specific NE-mediated release of the MMAE payload **9** in TME. Further investigations of dose and schedule as well as characterization of safety, ADME properties and efficacy in patient-derived tumor models are warranted.

4.4 CDK-9i

Another payload class which attracted our interest was inhibitors of CDK-9. Advanced clinical compounds such as atuvaciclib (Lücking et al., 2017) and enitociclib (Lücking et al.,

2021) have shown promising activity for the treatment of hematological malignancies. We envisioned the sulfoximine group present in CDK-9i, such as atuvaciclib and enitociclib, as potential linker attachment site. The successful conversion of sulfoximines to pseudopeptides was described previously (Bolm et al., 1997). We chose to investigate the sulfoximines as the attachment site for NE-cleavable substrate peptides and their utility as part of NE-cleavable SMDCs. To explore treatment options also for solid tumors with $\alpha\beta 3$ -targeted CDK-9i SMDCs, we considered a highly potent subclass of macrocyclic CDK-9i such as **8**, which retains the atuvaciclib core. Synthesis of the $\alpha\beta 3$ -targeted SMDC **3** was successfully accomplished, and this SMDC, with a sulfoximide bond as linkage between payload and linker, met our criteria for efficient NE-mediated cleavage, NE-dependent cytotoxicity as well as high stability in plasma. In comparison to the other SMDCs described here, compound **3** showed a higher ratio of released payload compared with the parent SMDC in pharmacokinetic studies in rat as described in Section 3.6. When pharmacokinetic studies were performed in NCI H69 tumor bearing mice, a 7.6-fold higher exposure of released payload **8** was detected in the tumor *versus* plasma, indicating a successful delivery of the free payload to tumor tissue. These results validate the use of a sulfoximide linker as a new NE-cleavable functionality in drug conjugates. Further optimization is ongoing to demonstrate an *in vivo* proof of sulfoximide-linked CDK-9i as payloads in SMDCs for treatment of solid tumors.

4.5 KSPi

Kinesin spindle protein inhibitors (KSPi) have been successfully employed as payloads in ADCs, particularly when releasing a non-permeable metabolite modified with a CellTrapper moiety enabling tumor accumulation after intracellular cleavage (Kirchhoff et al., 2020). For utilization of KSPi payloads in SMDCs with extracellular cleavage, the physicochemical profile of the KSPi needs to be tuned for a different profile with high potency and a higher membrane permeability. The amino group present in KSPis may allow for the attachment of substrate sequences potentially cleaved by NE. Cleavability by NE would be a requirement, as this amino group has previously been shown to be essential for activity (Lerchen et al., 2018). The initially identified KSPi payload **10** was highly potent, but it also showed a high active efflux (Table 1 and 2). On top of this, the corresponding amide linked SMDC **5** showed only very slow and inefficient release of the payload **10** in the biochemical NE cleavage assay (Figure 3). Interestingly, inserting an N-methyl carboxamide moiety next to the amino group resulted in KSPi **11**, which was equipotent to **10** (Table 1) but had a significantly improved physicochemical profile with higher permeability and reduced efflux (Section. 3.5; Table 2). The corresponding SMDC **6** with a NE-cleavable linker attached to the amino group of the payload **11** also showed a significantly improved cleavability by NE *versus* **5**. Consequently, this optimized SMDC **6** was highly efficacious and well tolerated in the NCI H69 xenograft model with two doses of 40 mg/kg given i. v. once weekly. This initial data confirms successful delivery of KSPi to tumors with potentially less frequent dosing schedules than required for small molecule KSPis, such as ispinesib (Purcell et al., 2010). Furthermore, the

lack of exposure of systemically cleaved payload **11** after i. v. administration of the SMDC **6** to rat (Figure 4E) and no significant body weight loss observed in the *in vivo* studies demonstrate the potential of SMDCs with KSPi payloads such as **6** for high efficacy with lower side effects.

5 Conclusion

We have presented three case studies of $\alpha\text{v}\beta 3$ -targeted SMDCs, **2**, **4** and **6**, which demonstrate the versatile utility of NE-cleavable linkers in SMDCs. High stability of the SMDCs *in vitro* and *in vivo* combined with efficient cleavage by NE resulted in high NE-dependent cytotoxicity. Initial efficacy data in xenograft models showed tumor regression with good tolerability demonstrating the utility of this approach for selective delivery of payloads to the TME. These studies highlight the broader scope of potential payloads and tolerated conjugation chemistries paving the way for future SMDCs harnessing the safety features of $\alpha\text{v}\beta 3$ -targeted delivery approaches in combination with NE-mediated cleavage in the TME.

Data availability statement

The original contributions presented in the study are included in the article/Supplementary Material, further inquiries can be directed to the corresponding author.

Ethics statement

Ethical approval was not required for the studies on humans in accordance with the local legislation and institutional requirements because only commercially available established cell lines were used. The animal study was approved by the Regional Council Committee on the Ethics of Animal Experiments. The study was conducted in accordance with the local legislation and institutional requirements.

Author contributions

A-SR: Writing–original draft, Writing–review and editing, Conceptualization, Investigation, Methodology. MW: Conceptualization, Writing–original draft, Writing–review and editing. BS-L: Conceptualization, Investigation, Methodology, Writing–original draft, Writing–review and editing. HW: Writing–original draft, Writing–review and editing, Methodology. AJ: Writing–original draft, Writing–review and editing. RI:

Writing–original draft, Writing–review and editing. AH: Writing–original draft, Writing–review and editing, Funding acquisition, Supervision. H-GL: Supervision, Writing–original draft, Writing–review and editing, Conceptualization, Methodology, Project administration.

Funding

The author(s) declare no financial support for the research, authorship, and/or publication of this article.

Acknowledgments

We thank DiBetta, A.-M., Graewinger, K., Koenig, B., Reimer, K., and Siefert, C. for excellent technical assistance and Koebberling, J. for the supervision. We thank Nuvisan ICB, and, particularly, Erkelenz, M., Siemeister, G., Litztenburger, U., Reuvers, M., Behrens, D., Schmidt, T., and Stöckigt, D. for performing *in vitro*, *in vivo* and DMPK studies. We also thank Tshithenge, D., Spang, R., Voits, P., and Stoltefuss, M. for thoughtful analytical support and Lerchen, A. for planning and coordinating the synthesis of CDK-9i payloads.

Conflict of interest

Authors A-SR, MW, BS, H-GL were employed by Vincerox Pharma GmbH. Authors AJ, RI, and AH were employed by Vincerox Pharma, Inc. Author HW was a consultant for Vincerox Pharma Inc.

Publisher's note

All claims expressed in this article are solely those of the authors and do not necessarily represent those of their affiliated organizations, or those of the publisher, the editors and the reviewers. Any product that may be evaluated in this article, or claim that may be made by its manufacturer, is not guaranteed or endorsed by the publisher.

Supplementary material

The Supplementary Material for this article can be found online at: <https://www.frontiersin.org/articles/10.3389/fphar.2024.1358393/full#supplementary-material>

References

- Achilles, K., and Bednarski, P. J. (2003). Quantification of elastase-like activity in 13 human cancer cell lines and in an immortalized human epithelial cell line by RP-HPLC. *Biol. Chem.* 384 (5), 817–824. doi:10.1515/BC.2003.091
- Alday-Parejo, B., Stupp, R. C., and Rüegg, C. (2019). Are integrins still practicable targets for anti-cancer therapy? *Cancers* 11, 978. doi:10.3390/cancers11070978
- Alloatti, D., Giannini, G., Vesci, L., Castorina, M., Pisano, C., Badaloni, E., et al. (2012). Camptothecins in tumor homing via an RGD sequence mimetic. *Bioorg. Med. Chem. Lett.* 22 (20), 6509–6512. doi:10.1016/j.bmcl.2012.07.061
- Baah, S., Laws, M., and Rahman, K. M. (2021). Antibody–drug conjugates—a tutorial review. *Molecules* 26 (10), 2943. doi:10.3390/molecules26102943

- Bennett, G., Brown, A., Mudd, G., Huxley, P., Van Rietschoten, K., Pavan, S., et al. (2020). MMAE delivery using the bicyclic toxin conjugate BT5528. *Mol. Cancer Ther.* 19 (7), 1385–1394. doi:10.1158/1535-7163.MCT-19-1092
- Bolm, C., Kahmann, J. D., and Moll, G. (1997). Sulfoximines in pseudopeptides. *Tetrahedron Lett.* 38 (7), 1169–1172. doi:10.1016/s0040-4039(97)00001-4
- Carl, P. L., Chakravarty, P. K., and Katzenellenbogen, J. A. (1981). A novel connector linkage applicable in prodrug design. *J. Med. Chem.* 24 (5), 479–480. doi:10.1021/jm00137a001
- Cazzamalli, S., Dal Corso, A., Widmayer, F., and Neri, D. (2018). Chemically-defined antibody- and small molecule-drug conjugates for *in vivo* tumor targeting applications: a comparative analysis. *J. Am. Chem. Soc.* 140 (5), 1617–1621. doi:10.1021/jacs.7b13361
- Danen, E. H., Ten Berge, P. J., Van Muijen, G. N., Van 't Hof-Grootenboer, A. E., Bröcker, E. B., and Ruiter, D. J. (1994). Emergence of alpha 5 beta 1 fibronectin- and alpha v beta 3 vitronectin-receptor expression in melanocytic tumour progression. *Histopathology* 24 (3), 249–256. doi:10.1111/j.1365-2559.1994.tb00517.x
- Davies, B., and Morris, T. (1993). Physiological parameters in laboratory animals and humans. *Pharm. Res.* 10 (7), 1093–1095. doi:10.1023/a:1018943613122
- Davis, R. A., Ganguly, T., Harris, R., Hausner, S. H., Kovacs, L., and Sutcliffe, J. L. (2023). Synthesis and evaluation of a monomethyl auristatin E-Integrin $\alpha\text{V}\beta\text{6}$ binding peptide-drug conjugate for tumor targeted drug delivery. *J. Med. Chem.* 66 (14), 9842–9852. doi:10.1021/acs.jmedchem.3c00631
- Dharmaratne, N. U., Kaplan, A. R., and Glazer, P. M. (2021). Targeting the hypoxic and acidic tumor microenvironment with pH-sensitive peptides. *Cells* 10 (3), 541. doi:10.3390/cells10030541
- Hatley, R. J. D., Macdonald, S. J. F., Slack, R. J., Le, J., Ludbrook, S. B., and Lukey, P. T. (2018). An αv -RGD integrin inhibitor toolbox: drug discovery insight, challenges and opportunities. *Angew. Chem. Int. Ed.* 57 (13), 3298–3321. doi:10.1002/anie.201707948
- Hieken, T. J., Farolan, M., Ronan, S. G., Shilkaitis, A., Wild, L., and Gupta, T. K. D. (1996). Beta3 integrin expression in melanoma predicts subsequent metastasis. *J. Surg. Res.* 63 (1), 169–173. doi:10.1006/jsr.1996.0242
- Kirchhoff, D., Stelte-Ludwig, B., Lerchen, H. G., Wengner, A. M., Ahsen, O. v., Buchmann, P., et al. (2020). IL3RA-Targeting antibody–drug conjugate BAY-943 with a kinesin spindle protein inhibitor payload shows efficacy in preclinical models of hematologic malignancies. *Cancers* 12, 3464. doi:10.3390/cancers12113464
- Korkmaz, B., Moreau, T., and Gauthier, F. (2008). Neutrophil elastase, proteinase 3 and cathepsin G: physicochemical properties, activity and physiopathological functions. *Biochimie* 90 (2), 227–242. doi:10.1016/j.biochi.2007.10.009
- Kunimoto, T., Nitta, K., Tanaka, T., Uehara, N., Baba, H., Takeuchi, M., et al. (1987). Antitumor activity of 7-Ethyl-10-[4-(1-piperidino)-1-piperidino]carbonyloxycamptothecin, a novel water-soluble derivative of camptothecin, against murine tumors. *Cancer Res.* 47 (22), 5944–5947.
- Lerchen, H.-G., Wittrock, S., Stelte-Ludwig, B., Sommer, A., Berndt, S., Griebenow, N., et al. (2018). Antibody–drug conjugates with pyrrole-based KSP inhibitors as the payload class. *Angew. Chem. Int. Ed.* 57 (46), 15243–15247. doi:10.1002/anie.201807619
- Lerchen, H. G., Stelte-Ludwig, B., Heroult, M., Zubov, D., Gericke, K. M., Wong, H., et al. (2023). Discovery of VIP236, an $\alpha\text{V}\beta\text{3}$ -targeted small-molecule–drug conjugate with neutrophil elastase-mediated activation of 7-ethyl camptothecin payload for treatment of solid tumors. *Cancers* 15 (17), 4381. doi:10.3390/cancers15174381
- Lerchen, H. G., Stelte-Ludwig, B., Kopitz, C., Heroult, M., Zubov, D., Willuda, J., et al. (2022). A small molecule–drug conjugate (SMDC) consisting of a modified camptothecin payload linked to an $\alpha\text{V}\beta\text{3}$ binder for the treatment of multiple cancer types. *Cancers (Basel)* 14 (2), 391. doi:10.3390/cancers14020391
- Liu, Y., Bajjuri, K. M., Liu, C., and Sinha, S. C. (2012). Targeting cell surface $\alpha\text{v}\beta\text{3}$ increases therapeutic efficacies of a legumain protease-activated auristatin prodrug. *Mol. Pharm.* 9 (1), 168–175. doi:10.1021/mp200434n
- Lücking, U., Kosemund, D., Böhnke, N., Lienau, P., Siemeister, G., Denner, K., et al. (2021). Changing for the better: discovery of the highly potent and selective CDK9 inhibitor VIP152 suitable for once weekly intravenous dosing for the treatment of cancer. *J. Med. Chem.* 64 (15), 11651–11674. doi:10.1021/acs.jmedchem.1c01000
- Lücking, U., Scholz, A., Lienau, P., Siemeister, G., Kosemund, D., Bohlmann, R., et al. (2017). Identification of atuviciclib (BAY 1143572), the first highly selective, clinical PTEFb/CDK9 inhibitor for the treatment of cancer. *ChemMedChem* 12 (21), 1776–1793. doi:10.1002/cmdc.201700447
- Ludwig, B. S., Kessler, H., Kossatz, S., and Reuning, U. (2021). RGD-binding integrins revisited: how recently discovered functions and novel synthetic ligands (Re-)Shape an ever-evolving field. *Cancers* 13 (7), 1711. doi:10.3390/cancers13071711
- Lulla, A. R., Akli, S., Karakas, C., Caruso, J. A., Warma, L. D., Fowlkes, N. W., et al. (2023). Neutrophil elastase remodels mammary tumors to facilitate lung metastasis. *Mol. Cancer Ther.*, OF1–OF15. Online ahead of print. doi:10.1158/1535-7163.MCT-23-0414
- Paulus, J., Nachtigall, B., Meyer, P., and Sewald, N. (2023). RGD peptidomimetic MMAE-conjugate addressing integrin $\alpha\text{V}\beta\text{3}$ -expressing cells with high targeting index. *Chem. – A Eur. J.* 29 (12), e202203476. doi:10.1002/chem.202203476
- Paulus, J., and Sewald, N. (2022). Synthesis and evaluation of a non-peptide small-molecule drug conjugate targeting integrin $\alpha\text{V}\beta\text{3}$. *Front. Chem.* 10, 869639. doi:10.3389/fchem.2022.869639
- Perrier, D., and Gibaldi, M. (1982). General derivation of the equation for time to reach a certain fraction of steady state. *JPharmSci* 71 (4), 474–475. doi:10.1002/jps.2600710432
- Powers, J. C., Gupton, B. F., Harley, A. D., Nishino, N., and Whitley, R. J. (1977). Specificity of porcine pancreatic elastase, human leukocyte elastase and cathepsin G inhibition with peptide chloromethyl ketones. *Biochimica Biophysica Acta (BBA) - Enzym.* 485 (1), 156–166. doi:10.1016/0005-2744(77)90203-0
- Purcell, J. W., Davis, J., Reddy, M., Martin, S., Samayoa, K., Vo, H., et al. (2010). Activity of the kinesin spindle protein inhibitor ispinesib (SB-715992) in models of breast cancer. *Clin. Cancer Res.* 16 (2), 566–576. doi:10.1158/1078-0432.CCR-09-1498
- Raposo Moreira Dias, A., Pina, A., Dean, A., Lerchen, H., Caruso, M., Gasparri, F., et al. (2019). Neutrophil elastase promotes linker cleavage and paclitaxel release from an integrin-targeted conjugate. *Chemistry* 25 (7), 1696–1700. doi:10.1002/chem.201805447
- Sato, T., Takahashi, S., Mizumoto, T., Harao, M., Akizuki, M., Takasugi, M., et al. (2006). Neutrophil elastase and cancer. *Surg. Oncol.* 15 (4), 217–222. doi:10.1016/j.suronc.2007.01.003
- Schwab, D., Fischer, H., Tabatabaei, A., Poli, S., and Huwyler, J. (2003). Comparison of *in vitro* P-glycoprotein screening assays: recommendations for their use in drug discovery. *J. Med. Chem.* 46 (9), 1716–1725. doi:10.1021/jm021012t
- Schwartz, R. S. (2004). Paul Ehrlich's magic bullets. *N. Engl. J. Med.* 350 (11), 1079–1080. doi:10.1056/NEJMp048021
- Seelig, A. (2020). P-glycoprotein: one mechanism, many tasks and the consequences for pharmacotherapy of cancers. *Front. Oncol.* 10, 576559. doi:10.3389/fonc.2020.576559
- Senter, P. D., and Sievers, E. L. (2012). The discovery and development of brentuximab vedotin for use in relapsed Hodgkin lymphoma and systemic anaplastic large cell lymphoma. *Nat. Biotechnol.* 30 (7), 631–637. doi:10.1038/nbt.2289
- Singh, S. B. (2022). Discovery and development of dolastatin 10-derived antibody drug conjugate anticancer drugs. *J. Nat. Prod.* 85 (3), 666–687. doi:10.1021/acs.jnatprod.1c01135
- Sun, F., Wang, J., Sun, Q., Li, F., Gao, H., Xu, L., et al. (2019). Interleukin-8 promotes integrin β3 upregulation and cell invasion through PI3K/Akt pathway in hepatocellular carcinoma. *J. Exp. Clin. Cancer Res.* 38 (1), 449. doi:10.1186/s13046-019-1455-x
- Troutman, M. D., and Thakker, D. R. (2003). Novel experimental parameters to quantify the modulation of absorptive and secretory transport of compounds by P-glycoprotein in cell culture models of intestinal epithelium. *Pharm. Res.* 20 (8), 1210–1224. doi:10.1023/a:1025001131513
- Wu, C. M., Li, T. M., Tan, T. W., Fong, Y. C., and Tang, C. H. (2013). Berberine reduces the metastasis of chondrosarcoma by modulating the $\alpha\text{v}\beta\text{3}$ integrin and the PKC δ , c-src, and AP-1 signaling pathways. *Evidence-Based Complementary Altern. Med.* 2013, e423164. doi:10.1155/2013/423164
- Zambra, M., Randelović, I., Talarico, F., Borbély, A., Svajda, L., Tóvári, J., et al. (2023). Optimizing the enzymatic release of MMAE from isoDGR-based small molecule drug conjugate by incorporation of a GPLG-PABC enzymatically cleavable linker. *Front. Pharmacol.* 14, 1215694. doi:10.3389/fphar.2023.1215694
- Zhuang, C., Guan, X., Ma, H., Cong, H., Zhang, W., and Miao, Z. (2019). Small molecule-drug conjugates: a novel strategy for cancer-targeted treatment. *Eur. J. Med. Chem.* 163, 883–895. doi:10.1016/j.ejmech.2018.12.035